

Relaxational Singularities of Human Motor System at Aging Due to Short-Range and Long-Range Time Correlations

Renat Yulmetyev

*Department of Physics, Kazan State University,
18 Kremlevskaya Str., 420008 Kazan, RUSSIA **

David E. Valliancourt

School of Kinesiology, University Illinois at Chicago, Chicago, Illinois, 60608 USA

Fail Gafarov

*Department of Theoretical Physics, Kazan State Pedagogical
University, 1 Mezhlauk Str., 420021 Kazan, RUSSIA*

Peter Hänggi

*Department of Physics, University of Augsburg,
Universitätsstrasse 1, D-86135 Augsburg, GERMANY*

(Received 20 January 2006)

In this paper we study the relaxation singularities of human motor system at aging. Our purpose is to examine the structure of force output variability as a function of human aging in the time and frequency domains. For analysis of experimental data we have developed here the statistical theory of relaxation of force output fluctuation with taking into account the effects of two relaxation channels. One of them contains the contribution of short-range correlation whereas other relaxation component reflects the effect of long-range correlation. The analysis of experimental data shows, that the general behavior of relaxation processes at human aging is determined by a complex combination and nonlinear interactions two above stated relaxation processes as a whole.

PACS numbers: 02.50. Wp, 02.50.-r, 05.20.-y, 05.65.+b, 45.05.+x, 45.65.+g, 87.*, 89.75.Fb, 95.75.Wx

Keywords: human aging, discrete non-Markov processes, statistical memory, short-time and long-time relaxation channels

1. Introduction

Recent studies the aging of human neuromuscular system has focused on application of central theory regarding the age relating with the structure of behavioral and physiological variability due to loss of "complexity"[1]-[3]. The term of "complexity" is connected to the broader concept including the fractals and dynamics

in disease and aging. The concept consider behavioral and physiological changes of the system's due to aberrations in their time and frequency structure. However it is necessary to specify that less attention has been given to the neuromuscular changes associated with the time-dependent and dynamic peculiarities of force control till now.

In this study, we examine the time and frequency structure of healthy adult humans to determine a relaxation singularities, arising with aging of human motor systems. It is well known that aging tends to induce a range of performance

*Also at Department of Theoretical Physics, Kazan State Pedagogical University, 1 Mezhlauk Str., 420021 Kazan, RUSSIA

decrements in human motor system. A common finding is that the amount of motor variability increases in the healthy aging adult over a broad set of tasks [4]-[7].

Although consideration of the amount of variability is an important indicator of the aging neuromuscular system, the structure of motor variability also provides significant insight into system organization and human motor control [8]-[11]. The presence of short-time and long-range correlations in neuromuscular fluctuations in health has implications for understanding and mathematical modelling of neuroautonomic regulation. Here we have applied correlation analysis to assess the effects of physiological aging on correlation behavior of human motor system. The purpose of this paper was to consider the effects of aging and task demand on the relaxation structure of the signals of force output variability from the point of view of modern statistical physics. We consider the force-time series data as a discrete stochastic process and apply the statistical theory of non-Markov random processes in complex systems [12]-[15]. Therefore we can use the notions, based on the theory of chaos and information, in our analysis of complex systems. This allows to apply in our consideration representations and notions on statistical short-time and long-time memory, information measures of chaoticity or robustness, relaxation and kinetic parameters from statistical theory.

2. Methods

2.1. Participants

A total of 29 participants were assigned to three different age groups: young group (N=10; range: 20-24 yrs; mean: 22 ± 1 yrs; 5 females and 5 males), old group (N=9; range: 64-69 yrs; mean: 67 ± 2 yrs; 4 females and 5 males), and older-old group (N=10; range: 75-90 yrs; mean: 82 ± 5 yrs; 5 females and 5 males). All of the participants were right hand dominant. The participants were

familiarized with the purpose of the experiment and all participants gave informed consent to all experimental procedures, which were approved by the local Institutional Review Board.

The three age groups consisted of moderately active individuals. Persons who were highly active were excluded from the study. Also, elderly persons who were considered frail were excluded from the study. Twelve of the participants in the two elderly groups were taking medication for the treatment of high blood pressure. The distribution of persons taking medication for high blood pressure was 8 in the older-old group and 4 in the old group. None of the elderly participants reported having a neuromuscular or neuropsychiatric disease, nor did any of the participants have diabetes. Also, twelve of the elderly participants reported having arthritis and each were taking medication for the condition. The distribution of persons reporting arthritis of the hand was 7 in the older-old group and 5 in the old group. All participants remained on their normal medications during testing.

2.2. Apparatus

Participants were seated in a chair with their dominant forearm resting on a table (75 cm in height). The participant's dominant hand was pronated and lay flat on the table with the digits of the hand comfortably extended. The setup constrained the wrist and the third, fourth and fifth phalanges from moving. The elbow position remained constant throughout the experimental session. Through abduction, the participant's lateral side of the index finger contacted the load cell (Entran ELFS-B3, New Jersey), 1.27 cm in diameter, which was fixated to the table. The load cell was located 36 cm from the participant's body midline. Analog output from the load cell was amplified through a Coulbourn Type A (Strain gauge Bridge) S72-25 amplifier at an excitation voltage of 10 V and a gain of 100. A computer controlled 16-bit A/D converter sampled the force output at 100 Hz. The smallest

increment of change in force the A/D board could detect was .0016 N. The force output was displayed on a video monitor located 48.6 cm from the participants' eyes and 100 cm from the floor. According to previous work from laboratory (D.A.V.), the display-to-control gain was set at 20 pixels per 1 N change in force for each participant.

2.3. Procedures

During the initial portion of the experiment, the participant's maximum voluntary contraction (MVC) was estimated consistent with previous work [7]. Participants abducted their index finger against the load cell with maximal force for three consecutive 6 s trials. A 60 s rest period was provided for each participant between each MVC trial. In each MVC trial, the mean of the greatest ten force samples was calculated. The means obtained from three trials were averaged to provide an estimate of each participant's MVC. Participants adjusted their level of force output to match a red target line (1 pixel thick) on the video monitor. Participants viewed online feedback of their performance in the form of a yellow force-time trajectory that moved from left to right in time across the video monitor. They were instructed to match the yellow trajectory line to the red horizontal target line throughout each trial, and to minimize all deviations of the yellow line from the red line.

Participants produced force at a constant force target. The constant target was a horizontal line displayed across the center of the video monitor. Participants produced force at 5, 10, 20 and 40 % of their MVC under the constant force condition for two consecutive 25 s trials at each force level. A rest period of 100 s was provided between each force trial. The order of the force and target conditions was randomized across all participants.

3. Data Analysis

The force-time series data were conditioned by the following methods. First, force data were digitally filtered by using a first-order Butterworth filter with a low-pass cutoff frequency of 20 Hz. All data processing and subsequent time and frequency analysis were performed by using software written in Matlab. The analysis of force output concentrated on two primary problems: 1) calculation of the information measure of chaosity or robustness of force variability; 2) study of the correlation and relaxation structure of force time variability.

3.1. The information measure of chaosity of force variability.

The quantitative information measure of chaosity of force variability was assessed by calculating of the statistical spectrum of non-Narkovity parameter (NMP). The equation

$$\varepsilon_i(\omega) = \left\{ \frac{\mu_i(\omega)}{\mu_i(\omega)} \right\}^{\frac{1}{2}}, \quad (1)$$

where $i = 1, 2, 3, \dots$ is the number of relaxation levels in kinetic description [12] of the time series, allow to calculate NMP ε_i from the power spectra of memory function of i th order $\mu_i(\omega)$. The mathematical procedure for a finding of $\mu_i(\omega)$ consist in calculation

$$\mu_i(\omega) = \tau^2 \left| \sum_{j=0}^{n-1} M_i(j\tau) \cos(j\omega\tau) \right|^2, \quad (2)$$

where $M_i(t)$ ($t = j\tau$) is the memory function of i th order, $\omega = 2\pi/\tau$, $\tau = 0,01s$ is the discretization time, n is the number of signals in time series. Memory functions, phase portraits of the dynamical orthogonal variables, and set of dynamical orthogonal variables of junior orders were calculated by the methods of well-known statistical theory of stochastic discrete non-Markov processes in complex systems with applications to cardiology, seismology, physiology

etc. The full details of the theory have been described elsewhere [12]-[15].

3.2. The correlation and relaxation analysis of force variability.

The structure of correlation and relaxation processes in force variability will be examined by using time and frequency analysis of correlation and studied relaxation processes. Correlation and relaxation rates for the short-range $R_i^{(s)}$ ($R_i^{(s)} = |\lambda_i|$, $i = 1, 2$) and long-range $R_i^{(l)}$ ($R_i^{(l)} = |\Lambda_i|^{1/2}$, $i = 1, 2$) relaxation (correlation) were used to consider the force signal. We shall calculate a general relaxation time in a frame of relaxation theory developed below.

Let's consider the structure of the initial time correlation function $a(t)$ of the force output time series signals. It is convenient to consider the chain of interconnected equations for the TCF $a(t)$ in a frame of Zwanzig'-Mori's kinetic theory [12]-[15]

$$\frac{da(t)}{dt} = \lambda_1 a(t) - \Lambda_1 \int_0^t a(t-\tau) M_1(\tau) d\tau, \quad (3)$$

$$\frac{dM_1(t)}{dt} = \lambda_2 M_1(t) - \Lambda_2 \int_0^t M_1(t-\tau) M_2(\tau) d\tau.$$

Here, the parameter $|\lambda_i|$ and $|\Lambda_i|^{1/2}$ define the local and memory channel relaxation (correlation) rates on the i 'th relaxation levels, correspondingly. Parameters λ_i has the dimension of relaxation rate, and Λ_i has a dimension of a square of frequency.

The structure of correlation and relaxation processes in force variability will be examined by using time and frequency analysis of correlation and studied relaxation processes. Correlation and relaxation rates for the short-range $R_i^{(s)}$ ($R_i^{(s)} = |\lambda_i|$, $i = 1, 2$) and long-range $R_i^{(l)}$ ($R_i^{(l)} = |\Lambda_i|^{1/2}$, $i = 1, 2$) relaxation (correlation) were used to consider the force signal. We shall calculate a general relaxation time in a frame of relaxation theory developed below.

Let's consider the structure of the initial time correlation function $a(t)$ of the force output time series signal. It is convenient to consider the chain of interconnected equations for the TCF $a(t)$ in a frame of Zwanzig'-Mori's kinetic theory [12]-[15]

Let's consider a partial solution of system (3.3) when we can use the time-scale invariance idea [19] - [21], [22]

$$M_2(t) = M_1(t) \quad (4)$$

on the second relaxation level. It means the approximate equality of memory life-times on the first and second relaxation levels. The similar condition is carried out in many concrete cases. The condition (3.4) apply on our situation as we shall see later. Using the Laplace transform on the normalized TCF $a(t)$, memory functions $M_1(t)$ and $M_2(t)$:

$$\begin{aligned} \tilde{a}(s) &= \int_0^\infty dt e^{-st} a(t), \quad M_i(s) \\ &= \int_0^\infty dt e^{-st} M_i(t), \end{aligned} \quad (5)$$

one can obtain solution of Eqns.(4)

$$\begin{aligned} \tilde{M}_1(s) &= \frac{1}{2\Lambda_2} \\ &\times \{-(s + R_2) \pm \sqrt{(s + R_2)^2 + 4\Lambda_2}\}, \quad (6) \\ \tilde{a}(s) &= \{s + R_1 + \frac{\Lambda_1}{2\Lambda_2} [-(s + R_2) \\ &+ \sqrt{(s + R_2)^2 + 4\Lambda_2}]\}^{-1}, \end{aligned}$$

where $R_i = R_i^{(s)} = |\lambda_i|$, $i=1, 2$. If we determine the general relaxation time τ_R by the relation $\tau_R = \Re \lim_{s \rightarrow 0} \tilde{a}(s)$, where \Re means real part, the resulting general equations for τ_R consequently can be written as follows

$$\tau_R = \{R_1 + \frac{\Lambda_1}{2\Lambda_2} [\sqrt{4\Lambda_2 + R_2^2} - R_2]\}^{-1}, \quad (7)$$

if $4\Lambda_2 + R_2^2 \geq 0$. Then we receive the formula

$$\tau_R = \frac{R_1 - \frac{\Lambda_1}{2\Lambda_2} R_2}{(R_1 - \frac{\Lambda_1}{2\Lambda_2} R_2)^2 + \frac{\Lambda_1^2}{4\Lambda_2^2} |4\Lambda_2 + R_2^2|}, \quad (8)$$

for $\Lambda_2 < 0$, $4\Lambda + R_2^2 < 0$. We can consider also two limiting cases from general Eqn. (7)

$$\begin{aligned} a) R_2^2 \gg 4\Lambda_2, \Lambda_2 > 0, \tau_R &= (R_1 + \Lambda_1/R_1)^{-1}; \quad (9) \\ b) R_2^2 \ll 4\Lambda_2, \Lambda_2 > 0, \tau_R &= (R_1 + \Lambda_1/\Lambda_2^{1/2})^{-1}. \end{aligned} \quad (10)$$

The equations (7)-(10) are our new theoretical results and they allow to calculate a general relaxation time τ_R for the various relaxation scenario. One can see from Eqns. (7)-(10) that general relaxation behavior is defined by complex nonlinear interactions and combinations of short-range and long-range relaxation processes on the first and second relaxation levels. Therefore, the general behavior of relaxation time τ_R is determined by a complex combination of relaxation rates R_1 , R_2 , $|\Lambda_1|^{1/2}$ and $|\Lambda_2|^{1/2}$ on these two interconnected relaxation levels. Calculating these five relaxation parameters: τ_R , $\tau_1^{(s)} = R_1^{-1}$, $\tau_2^{(s)} = R_2^{-1}$, $\tau_1^{(l)} = |\Lambda_1|^{-1/2}$ and $\tau_2^{(l)} = |\Lambda_2|^{-1/2}$ we can receive a rather detailed and specific singularities of relaxation processes in a complex systems.

4. Results

Figure 1 shows force output from young (B), old (C), and older-old(D) participants at 20% MVC at the constant(t1) and sine wave (t2) targets. The amount of force variability was examined by calculating the root mean square error (see, for details [23]). Figure 2 depicts the values of short-range relaxation parameter on a first relaxation level λ_1 ($R_1 = |\lambda_1|$ is the corresponding relaxation rate) with following name structure

1 - s1c1t1	9 - s2c1t1	17 - s3c1t1
2 - s1c1t2	10 - s2c1t2	18 - s3c1t1
3 - s1c2t1	11 - s2c2t1	19 - s3c2t1
4 - s1c2t2	12 - s2c2t2	20 - s3c2t2
5 - s1c3t1	13 - s2c3t1	21 - s3c3t1
6 - s1c3t2	14 - s2c3t2	22 - s3c3t2
7 - s1c4t1	15 - s2c4t1	23 - s3c4t1
8 - s1c4t2	16 - s2c4t2	24 - s3c4t2

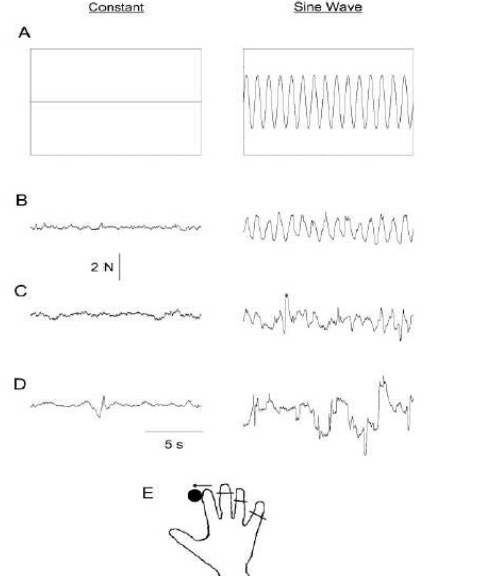


FIG. 1. Force output from young (B), old (C), and older-old(D) participants at 20% MVC at the constant(t1) and sine wave (t2) targets.

The file naming includes the experimental design AGE GROUP(3) \times FORCE LEVEL(4) \times TRIALS(2):

S1:group number s1-young (20-24 years), s2-old (64-69 years), s3-oldest old (75-90 years);

C1:force level (C1-5%, C2-10 %, C3-20 %, C4-40 %).

T1:trial number (t1-trial 1, t2-trial 2).

Each file contains 25 s force data (in Newtons) collected at 100 Hz ($\tau = 0,01s$). A more detailed description of the experiment and data collection is found in [23].

Figure 2 shows numerical values of parameter λ_1 for all three groups s1,s2, and s3. In Figure 2 the box lines at the lower quartile, median and upper quartile values. The whiskers are lines extending from end of the box to show the extent of the rest of the data. Outliers are data with values beyond the ends of the whiskers. We should add still, that first eight boxes correspond to s1 group (young), next eight boxes correspond to the second s2(old) group and last ones correspond to the third s3 group (oldest old).

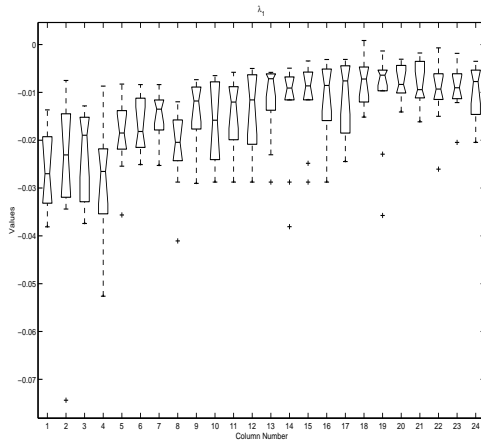


FIG. 2. Relaxation parameter due to short-range correlations λ_1 (or short-range relaxation rate $R_1^{(s)} = |\lambda_1|$) for the all studied groups at first relaxation level in units of τ^{-1} , where $\tau = 0,01$ s is a discretization time. The details of description and processing of statistical data see in text of the paper. Data testify for fast relaxation for young ($R_1^{(s)} = 0,02 \tau^{-1}$), more slow relaxation for old ($R_1^{(s)} = 0,01 \tau^{-1}$) and oldest old ($R_1^{(s)} = 0,007 \tau^{-1}$) groups. In a whole a difference for short-range relaxation rate for ratio of young / old constitute 1,8 times, for young / oldest old is 2,66 times and for old / oldest old is 1,44 times. In a separate cases last ratio constitute 3,47 and more times!

One can calculate from Fig. 2 that the mean value of parameter λ_1 for first s1 group is $\lambda_1 = -0,0203\tau^{-1}$, for second s2 group $\lambda_1 = -0,0110\tau^{-1}$, and for third s3 group of participants $\lambda_1 = -0,00763\tau^{-1}$. Similar distinction in rates and times of the short-range relaxation is quite explainable with the physiological points of view. We shall note, that the greatest distinction in young and old groups achieves 3,47 times. From physical point of view it means a more fast relaxation of the force fluctuation for young and more slower relaxation for old and oldest old.

Fig. 3 show a similar behavior of the second short-range relaxation parameter λ_2 for all studied groups of participants. Authentic appreciable distinction (in 2,11 times) in relaxation rates for young for force levels c1,

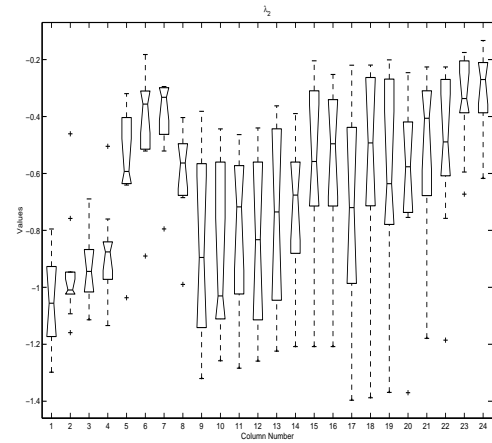


FIG. 3. Relaxation parameter λ_2 due to short-range correlation (rate of short-range relaxation $R_2^{(s)} = |\lambda_2|$) for the all studied groups at second relaxation level in units of τ^{-1} . For young group one can see a sharp decreasing of $R_2^{(s)}$ and λ_2 at high force levels (c3, c4). In the old group it is seen a steady decreasing of relaxation rate at raising of force level as for constant well as well for sine wave force output task. In oldest old group steady decreasing of $R_2^{(s)}$ is observed for constant force output task whereas for sine wave force output task a decreasing is definite less.

c2 and c3, c4 pays on itself attention. Average values R_2 in units of τ^{-1} in young group (0,778) and old (0,795) almost coincide with each other. Distinctions between force levels c1, c2 and c3, c4 in group oldest old is almost twofold. The greatest relaxation rate ($R_2 = 1,056\tau^{-1}$) is registered in young group at low force levels (c1, c2). The least relaxation rate is observed as for young group ($R_2 = 0,50\tau^{-1}$) at high force levels (c3, c4), and for oldest old group S3 ($R_2 = -0,36\tau^{-1}$) at high force levels (c4, c4).

The behavior of the third relaxation parameter λ_3 is displayed on Figure 4. Relaxation rate $R_3 = |\lambda_3|$ on the third relaxation a level is appeared, approximately, identical for the all three age groups.

Relaxation parameters Λ_1 and Λ_2 , connected with long-range time correlations, are shown in Figures 5 and 6 in units of τ_1 . Relaxation time ($\tau_1^{(l)} = |\Lambda_1|^{-1/2}$) for the first relaxation levels are

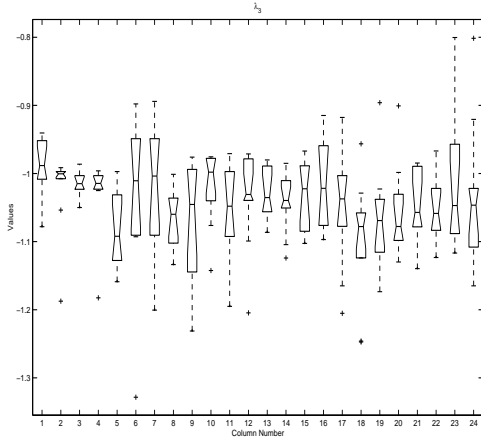


FIG. 4. Relaxation parameter λ_3 (rate of short-range relaxation $R_3^{(s)} = |\lambda_3|$) due short-range correlations for all studied groups at third relaxation level in units of τ^{-1} . One can observe almost invariable behavior of λ_3 for a s1,s2 and s3 groups. For a young group with enhancement of force level minimum $R_3^{(s)}$ is observed for force level c3 (20 %).

almost identical to all three age groups (s1, s2 and s3). It is necessary to note on appreciable distinction in group s1 of young participants force between low (c1, c2) ($\tau_2 = 0,71\tau$) and high (c3, c4) ($\tau_2 = 1,257\tau$) force levels. It testifies that long-range correlations mechanism of force relaxation, practically does not depend on age (average $\tau_1^{(l)}$ for groups s1, s2 and s3, are equal, respectively, $0,98\tau$; $1,16\tau$ and $0,98\tau$). Relaxation parameter Λ_2 turn out as negative for all three age groups s1, s2 and s3. This testify to a change of relaxation mode at the transition from the first on second relaxation levels. Relaxation times $\tau_2^{(l)}$ for groups s1, s2 and s3 changes slightly (they are equal $0,96\tau$; $0,79\tau$ and $1,11\tau$, correspondingly). It can testify upon the weak age changes in long-range relaxation mechanism of force output fluctuations.

On Fig. 7 one can see a values of non-Markovity parameter $\varepsilon_1(0)$ of the first relaxation level on zero frequency for three age groups s1, s2 and s3. Appreciable interest represent, that in young group (average value $\varepsilon_1 = 51,0$) and oldest old group ($\varepsilon_1 = 55,50$) the chaosity

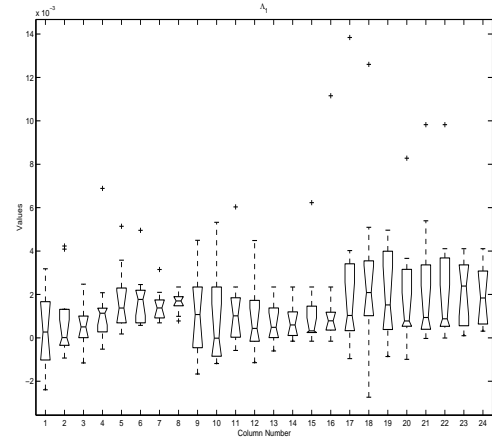


FIG. 5. Relaxation parameter due to long-range correlation Λ_1 (appropriate long-range relaxation rate $R_1^{(l)} = |\Lambda_1|^{-1/2}$) for s1, s2,s3 groups at first relaxation level in units of τ^{-2} . As parameter Λ_1 has a dimension of a square of frequency, parameter $R_i = |\Lambda_i|^{1/2}$ has a dimension of relaxation rate in units of τ^{-1} , where $\tau = 0,01\text{ s}$ is discretization time. One can see a steady increasing of this rate in four times for young group at constant force output task and twofold increasing for sine wave output task. For old group $R_1^{(l)}$ is steady for various force levels, in fact. Similar behavior of $R_1^{(l)}$ is remained for oldest old group in process of increase of force levels.

and randomness is approximately the same. Simultaneously it is obvious, that the greatest chaosity ($\varepsilon_1 = 107$) appears in group old participants s2. Fig. 8 presents statistical non-Markovity parameter on the second level $\varepsilon_2(0)$ for the all age groups. One can note, that everywhere $\varepsilon_2(0)$ is almost identical and equal unity. From results of Fig. 8 it follows, that a condition of applicability of time-scale invariance idea and approximate equality of memory life-time on the first and second relaxation levels (see, Eqn. (2)) is carried out with the high degree of accuracy. Because of the experimental data submitted on Fig. 8, one can use Eqns. (6) - (8) for calculation of general relaxation time τ_R .

Fig. 9 presents a values of time τ_R calculated according our theory, Eqns (6) - (8), for all studied groups of participants. Mean relaxation time for young group (s1) at enhancement of force level

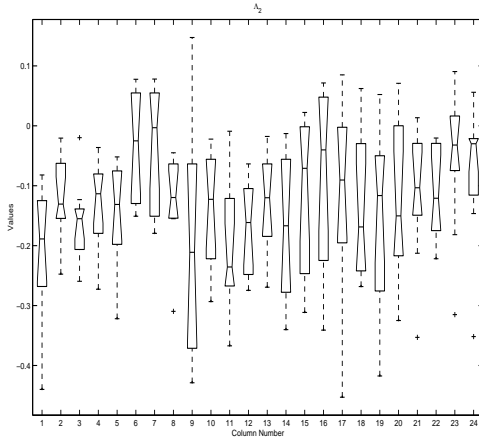


FIG. 6. Relaxation parameter due long-range correlation Λ_2 (of long-range relaxation rate $R_2^{(l)} = |\Lambda|^{1/2}$) for all studied groups s1, s2 and s3 at second relaxation level in units of τ^{-2} . One of the specific peculiarities of this case is a negative sign of parameter Λ_2 . It means a change of relaxation mode on the second relaxation level. For all studied groups s1,s2 and s3 we have approximately similar relaxation behavior. Consequently from the physical point of view one can suppose that contribution to relaxation due to long-range correlations is almost steady with aging.

(from c1, c2 to c3, c4) increase from value 42,5 τ up to value 56,07 τ . For the group of young mean τ_R is 49,3 τ , where as for the group of old and oldest old mean τ_R is equal 91,1 τ and 99,8 τ , correspondingly. It means, that a general relaxation time τ_R at ageing increase on two times, approximately.

Fig. 10 shows the phase portraits in a planes of four junior orthogonal dynamic random variables W_0 , W_1 , W_2 and W_3 , calculated according theory [12]-[14] for experimental file named sld4c1t2 as an example. These portraits appears symmetrical in planes: (W_1, W_2) , (W_1, W_3) and (W_2, W_3) . Slight deviation from this symmetry one can see for planes of junior variables (W_0, W_i) , $i=1,2,3$. Phase clouds are dense and concentrated.

Fig. 11 present phase portraits for file name sld4c4t1 of young participant sld4 at highest force level (40 %). One can note a significant

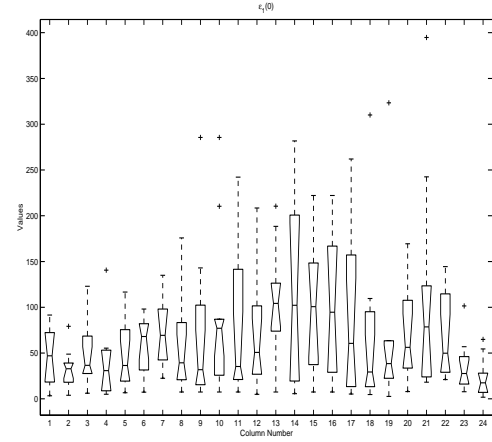


FIG. 7. First point of the statistical non-Markovity parameter $\varepsilon_1(0)$ on zero frequency $\omega = 0$ for groups s1, s2 and s3. Values of $\varepsilon_1(0)$ is approximately same for young ($\varepsilon_1 \sim 51$) and oldest old groups and $\varepsilon_1 \sim 107$ for old group. It means a similarity of quantitative measure of chaosity and randomness (existence of Markov effects) for these two groups (young and oldest old) and increase of this measure for all groups.

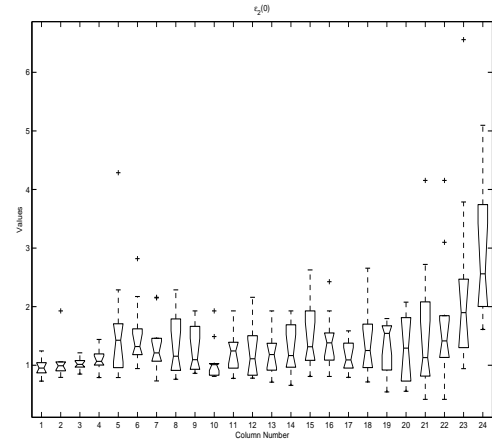


FIG. 8. Behavior of the second point of non-Markovity parameter $\varepsilon_2(0)$ in all studied groups s1, s2 and s3. One can see identical values of $\varepsilon_2(0) \sim 1$ with fine precision. Namely similar behavior let us to use a time scale-invariance idea and apply a solution (6)-(8) of kinetic equations (1)-(3) for analysis of experimental data. This figure constitute an experimental basis of our solution of kinetic equations for TCF and MF.

multifold swelling of volume of all phase clouds. This testify to the noticeable increasing of

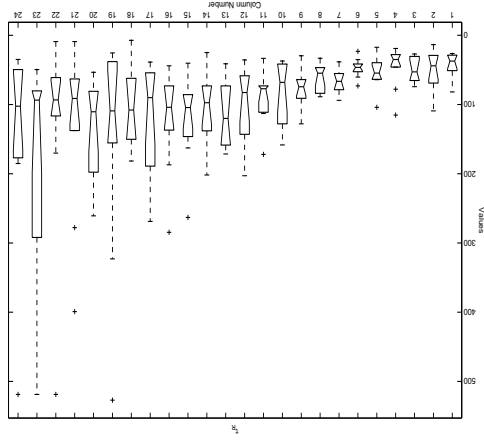


FIG. 9. General relaxation time τ_R , calculated in accordance with Eqns. (6)-(8) of our theory for all studied groups in units of τ . Aging appear as an approximate doubling of τ_R and slowdown of a whole relaxation process including as a short-range and well as a long-range correlations.

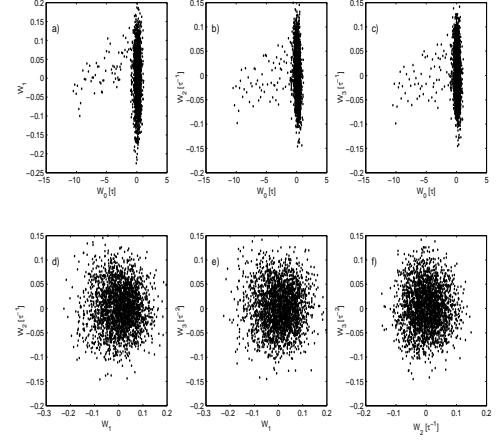


FIG. 11. Enhancement of force level (c4 instead of c1) for participant d4 from young group reduce the scattering and appearance asymmetry of distribution of phase points. Therefore, raising of force level and force capacity lead to the swelling of phase clouds and to increase of the disordering effects in phase space.

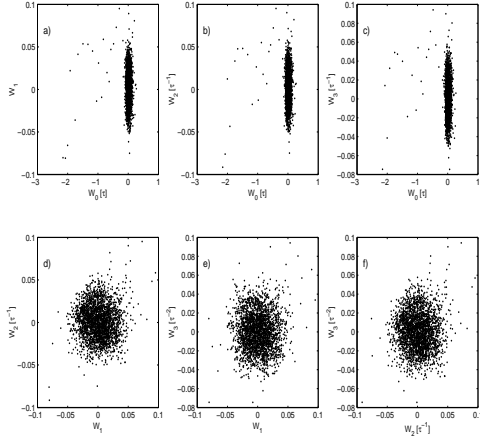


FIG. 10. Phase portraits in the planes (W_i, W_j) $i, j = 1, 2, 3$ of junior orthogonal dynamical variables W_i for participant d4 of young group at force level c1 and sine wave force output t2. One can characterize these portraits by a dense nucleus and small dissipation of phase points on the planes. Similar behavior is typical for healthy young human.

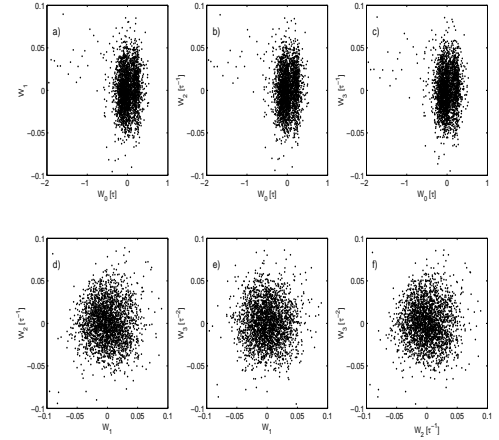


FIG. 12. Enhancement of force level (c4 instead of c1) for participant d4 from young group reduce the scattering and appearance asymmetry of distribution of phase points. Therefore, raising of force level and force capacity lead to the swelling of phase clouds and to increase of disordering dynamics in phase space.

chaosity of motor force activity for this case. Fig.12,13 depict a change of the structure of phase clouds for old participant s2d2 for force levels c1t2 and c4t4, as an example, correspondingly. On Fig.12 one can find the effect of condensation of all phase clouds. It correspond to lowest value

of the first non-Markovity parameter ($\varepsilon_1(0) \sim 18$) and weakly marked chaosity of force fluctuation. At the transition to other force level (4, 40 %) from Fig. 32a one can see the remarkable increasing of the volumes of all phase clouds and their appreciable asymmetry. It lead to increase

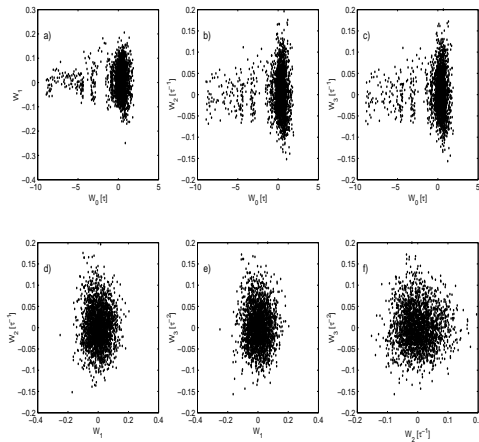


FIG. 13. Enhancement of force level (c4 instead of c1) for participant d2 of old group reduce to twofold swelling of phase clouds, remarkable stratification and scattering of phase points in phase space.

of chaosity of force fluctuation almost 7 times ($\varepsilon_1(0) = 120$).

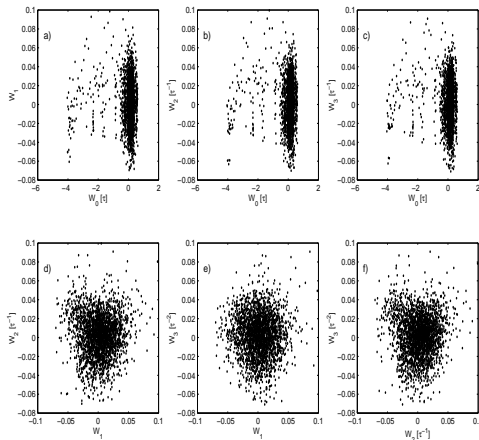


FIG. 14. Phase portraits in planes (W_i, W_j) $i, j = 1, 2, 3$ of junior dynamical orthogonal variables W_i for participant d8 of oldest old group at high level force c3 (20 %) and constant force output task (t1). Dense phase clouds (d,e,f) are accompanied by the slight stratification (see, figs a,b,c) of phase clouds.

Phase clouds for oldest old participants s3d8 for force levels c3t1 and c4t2 are shown on Figs. 14 and Figs.15, correspondingly. One can observe a change of distribution of phase points from consolidated ones (for planes (W_1, W_2) ,

(W_1, W_3) and (W_2, W_3)) to a more scattered distribution at transition from force state c3t1 to state c4t2. Simultaneously, a slight amplification of asymmetry of phase clouds in planes of junior variables (W_0, W_j) , $j=1,2,3$ occurs. Thus, a quantitative measure of chaosity $\varepsilon_1(0)$ on the first relaxation level does not vary almost (it equal 24 and 27, correspondingly). Therefore, the degree of Markovization and chaosity for these two cases does not change.

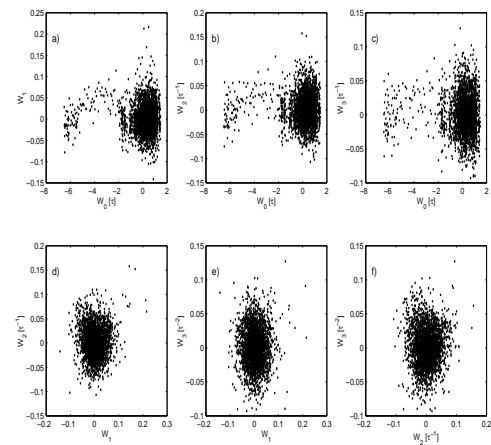


FIG. 15. Twofold enhancement of force level (c4 40 % instead of c3, 20 %) for participant d8 of oldest old group at sine wave force task reduce on minor change of the structure of phase portraits and phase clouds without any stratification and scattering of phase points in a phase space.

Figs. 16,17,18 demonstrate a frequency dependence of the first non-Markovity parameter $\varepsilon_1(\omega)$ for young (s1d5) old (s2d2) and oldest old (s3d2) participants in all force levels as an examples. From Fig.16 for participants s1d5 one can see that Markov effect at ultralow frequency remain constant at force level t1 (constant). At sine wave (e,f,g,h) force output task one can observe a progressive and steady decline of $\varepsilon_1(0)$ (from value of 50 on value of 8). It is connected with a reduction of Markov effects and steady amplification of non-Markov effects. Similar behavior of $\varepsilon_1(\omega)$ reflects the appearance of slight robustness in force fluctuation for young participants in process of increasing of force level.

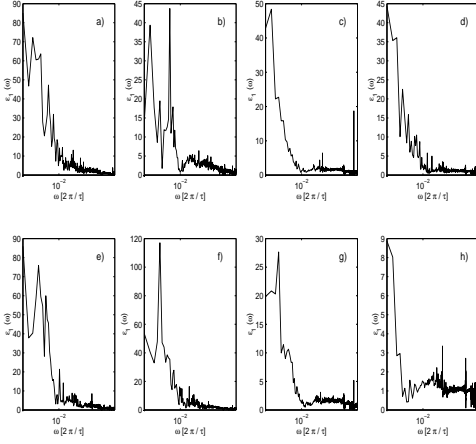


FIG. 16. Frequency dependence of the first point of non-Markovity parameter $\varepsilon_1(\omega)$ for participant d5 of young group for 8 trial: at four force levels (c1,c2,c3,c4) and at two form (t1, t2) of force output task. Data demonstrate almost invariable behavior of $\varepsilon_1(\omega)$ at constant force output task, and steady decreasing of quantitative measure of chaosity at sine wave force output task (for example, $\varepsilon_1(0)$ decrease from value of 40 to value of 8).

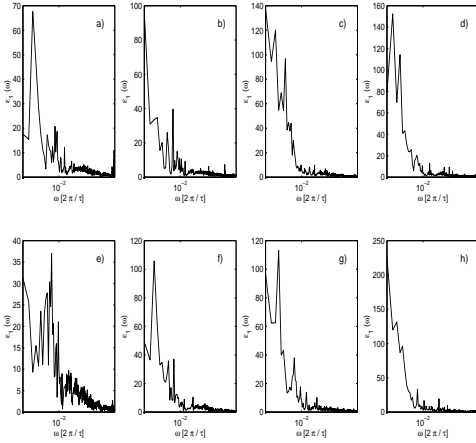


FIG. 17. Frequency dependence of the first point of non-Markovity parameter $\varepsilon_1(\omega)$ for participant d2 of old group for 8 trials: for force levels (5 %, 10 %, 20 % and 40 %) and two form (t1,t2) of force output task. Values of quantitative measure of chaosity ($\varepsilon_1(0)$) increase almost at ten times at constant force output task, whereas it increase almost at five times at sine wave force output task.

A data for old s2d2 presents opposite example, as can one see from Fig.17. We see

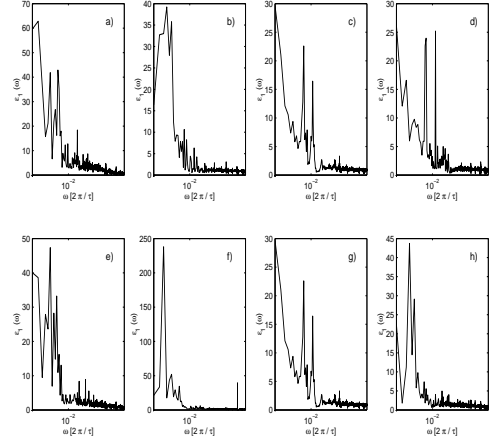


FIG. 18. Frequency dependence (a,b,c,d)of the first point of non-Markovity parameter $\varepsilon_1(\omega)$ for participant d2 of the oldest old group is related with the steady decreasing of quantitative measure of chaosity and randomness at enhancement of force level (5 %, 10 %, 20 % and 40 %) and constant force output task (t1). Similar behavior is observed for sine wave force output task (t2) also. Simultaneously, one can see low frequency range (from zero up to $10^{-2}Hz$) with the big values of $\varepsilon_1(\omega)$, that testify to the existence a steady frequency region of Markov random effects.

a drastic amplification of Markov effects in process of enhancement of force level for constant (a,b,c,d) and sine wave (e,f,g,h) force output task. This means a steady Markovization of a process, that is, a steady amplification of Markov random effects.

From Fig.18 one can note analogous behavior of $\varepsilon_1(\omega)$ for oldest old s3d2 at the constant (a,b,c,d) and sine wave (e-h) force output task. It testifies about a gradual and more distinctive display of non-Markov effects and robustness in force behavior for participant s3d2.

5. Discussion and conclusion

The purpose of this study was to examine the structure in the time and frequency domains of force output variability as a function of human aging.

For the analysis of force fluctuation we have

used the statistical relaxation singularities of motor system related to the short-range and long-range time correlation.

It is necessary to emphasize some fundamental points, following from the study. Force output dynamics for all three groups of healthy (young, old and oldest old) can be characterized rather a high level of chaoticity and randomness on the first relaxation level of force output fluctuation. For all files studied we have found out, that $\varepsilon_1(\omega)$ changes in a wide interval of values (7-300). It allows to state a strong chaotization and clearly expressed Markov effects for all healthy groups. As is known, beginning of illnesses, for example Parkinson disease (see, for instance, [18]) results to suppression of Markov effects and appearance of non-Markovity effects and robustness.

The same level of a randomness observed for young ($\varepsilon_1 \sim 51$) and oldest old ($\varepsilon_1 \sim 56$) turned out to be unexpected. Thus, on average the rather highest level of a randomness ($\varepsilon_1 \sim 107$) are registered in old group. These values of NMR (ε_1) signify healthy state for studied participants. Therefore it is possible to state with assurance that the information measure of a randomness is the greater for old, but it is smaller for young and oldest old groups. Steady non-Markovity ($\varepsilon_2 \sim 51$) on the second relaxation level for all three age groups confirms our supposition for the advantage of time-scale invariance idea of relaxation processes of force output fluctuation on these level.

The relaxation singularities of force output fluctuations consist in the following. At the first relaxation level a remarkable distinction of relaxation rates of force output fluctuation is observed. It means that relaxation related to the short-range correlation is a more fast at low force level. With the enhancement of force levels the relaxation is rather decelerated. Noticeably more slow relaxation appears in two old groups s2 and s3. Hence we can conclude

that aging becomes apparent as the notably slowing-down of relaxation processes, connected with the effect off the short-range correlation. In the second relaxation level contribution of short-range correlation for all age groups are the same. At that we notice stably (more than 2 times) decreasing of the relaxation rate with increasing of force level (from c1,c2 to c3,c4).

The following fact attract our steadfast attention. One can note, that contribution of long-range correlations in relaxation rates is, approximately, identical for the all three age groups and it does not depend on age on the first relaxation level. However, in young group here specific features are observed. They are that here relaxations rates increase, on the average, at 1,5 times at high force levels (c3 and c4). On the second relaxation level the similar picture is kept.

For analysis of experimental data we have developed here the statistical theory of relaxation of force output fluctuation with taking into account: first two relaxation levels and effects of two relaxation channels. One of the relaxation channel contains the contribution of short-range correlation whereas other component of relaxation reflects the effect of long-range correlation. The analysis of experimental data shows, that one can determine the general behavior of relaxation processes as a whole by a complex combination and nonlinear interaction of these two above stated relaxation processes.

Acknowledgments

This work was partially supported by the RFBR (Grants no. 05-02-16639-a), Grant of Federal Agency of Education of Ministry of Education and Science of Russian Federation. This work has been supported in part (P.H.) by the German Research Foundation, SFB-486, project A10.

References

- [1] Lipsitz Z. A., and Goldberger A. Z., Loss of "complexity" of cardiovascular dynamics: a potential marker of vulnerability to disease. *Chaos* **5**, 102-109 (1995).
- [2] Valliancourt D. E., and Newell K. M., Changing of complexity in human behaviour and physiology through aging and diseases. *Neurobiological Aging* **23**, 1-11 (2002).
- [3] Valliancourt D. E., and Newell K. M., Response to reviewers commentaries. *Neurobiological Aging* **23**, 27-29 (2002).
- [4] Goldanski M. E., Fuglevand A. J., and Enoka R. M., Reduced control of motor output in a human hand muscle of elderly participants during submaximal contractions. *J. Neurophysiol* **69**, 2108-2115 (1993).
- [5] Zaidlow D. H., Bilodeau M., and Enoka R. M., Steadiness is reduced and motor unit discharge is more variable in old adults. *Muscle Nerve* **23**, 600-612 (2000).
- [6] Tracy B. L., and Enoka R. M., Older adults are less steady during submaximal isometric contractions with the knee extensor muscles. *J. Appl. Physiology* **92**, 1004-1012 (2002).
- [7] Valliancourt D. E., Zarsson L., Newell K. M., Effects of aging on force variability, motor unit discharge patterns and the structure of 10, 20, and 40 Hz EMG activity. *Neurobiology of aging* **24**, 25-35 (2003).
- [8] Goldberger A. L., and West B. J., Fractals in physiology and medicine. *Yale J. Biol. Med.* **60**, 421-435 (1987).
- [9] Hausdorff J. M., Peng C. K., Ladin Z., Wei J. Y., and Goldberger A. L., Is walking a random walk? Evidence for long-range correlations in stride interval of human gait. *J. Appl. Physiol.* **78**, 349-358 (1994).
- [10] Kaplan D. T., Furman M. I., Pincus S. M., Ryan S. M., Lipsitz L. A., and Goldberger A. L., Aging and complexity of cardiovascular dynamics. *Biophys. J.* **59**, 945-949 (1991).
- [11] Newell K. M. and Corcos D. M. (Editors) Variability and motor control, Champaign, IL: Human Kinetics, 1993.
- [12] Yulmetyev R., Hänggi P., and Gafarov F., Stochastic dynamics of time correlation in complex systems with discrete current time. *Phys. Rev. E* **2000**, 62 (5). 6178-6194
- [13] Yulmetyev R., Gafarov F., Hänggi P., Nigmatullin R. and Kayumov S., Possibility between earthquake and explosion seismogram differentiation by discrete stochastic non-Markov processes and local Hurst exponent analysis. *Phys. Rev. E* **2001**, 64 (6). 066132
- [14] Yulmetyev R., Hänggi P., and Gafarov F., Quantification of heart rate variability by discrete non-stationary non-Markov stochastic processes. *Phys. Rev. E* **2002**, 65 (4). 046107
- [15] Yulmetyev R., Hänggi P., and Gafarov F., Stochastic processes of demarkovization in chaotic signals of human brain electric activity from EEG's during epilepsy. *JETP* **96**, 572-580 (2003).
- [16] Yulmetyev R. M., Gafarov F. M., Yulmetyeva D. G., Emeljanova N. A., Intensity approximation of random fluctuation in complex systems. *Physica A* **303**, 427-438 (2002).
- [17] Yulmetyev R. M., Emelyanova N. E., Peter Hänggi, Gafarov F. M., Prokhorov A. O., Long-range memory and non-Markov statistical effects in human sensorimotor coordination. *Physica A* **316**, 671-687 (2002).
- [18] Yulmetyev R., Demin S., Emelyanova N., Gafarov F., Hänggi P., Stratification of the phase clouds and statistical effects of the non-Markovity in chaotic time series of human gait for healthy people and Parkinson patients. *Physica A* **319**, 432-446 (2003).
- [19] Yulmetyev R. M., Mokshin A. V., Hänggi P., and Shurygin V. Yu., Time-scale invariance of relaxation processes of density fluctuation in slow neutron scattering in liquid cesium. *Phys. Rev. E* **64**, 057101 (2001).
- [20] Yulmetyev R. M., Mokshin A. V., Hänggi P., and Shurygin V. Yu., Dynamic structure factor in liquid cesium on the basis of time-scale invariance of relaxation processes. *JETP Lett.* **76**, 147 (2002).
- [21] Yulmetyev R. M., Mokshin A. V., Scopigno T., and Hänggi P., New evidence for the idea of timescale invariance of relaxation processes in simple liquids: the case of molten sodium. *J. Phys.: Condens. Matter* **15**, 2235-2257 (2003).
- [22] Ballucani U., Lee M. H., and Togneth V., Dynamical correlations. *Phys. Reports* **373**, 409-492 (2003).
- [23] Valliancourt D. E., Newell K. M., Aging and time and frequency structure of force output variability. *J. Appl. Physiol.* **94**, 903-912 (2003).